

Structure analysis for hole-nuclei close to ^{132}Sn by a large-scale shell-model calculation

Han-Kui Wang,¹ Yang Sun,^{1,2,*} Hua Jin,^{1,3} Kazunari Kaneko,⁴ and Shigeru Tazaki⁵

¹*Department of Physics and Astronomy, Shanghai Jiao Tong University, Shanghai 200240, People's Republic of China*

²*Institute of Modern Physics, Chinese Academy of Sciences, Lanzhou 730000, People's Republic of China*

³*Department of Mathematics and Physics, Shanghai Dianji University, Shanghai 200240, People's Republic of China*

⁴*Department of Physics, Kyushu Sangyo University, Fukuoka 813-8503, Japan*

⁵*Department of Applied Physics, Fukuoka University, Fukuoka 814-0180, Japan*

(Received 18 September 2013; published 13 November 2013)

The structure of neutron-rich nuclei with a few holes in respect of the doubly magic nucleus ^{132}Sn is investigated by means of large-scale shell-model calculations. For a considerably large model space, including orbitals allowing both neutron and proton core excitations, an effective interaction for the extended pairing-plus-quadrupole model with monopole corrections is tested through detailed comparison between the calculation and experimental data. By using the experimental energy of the core-excited $21/2^+$ level in ^{131}In as a benchmark, monopole corrections are determined that describe the size of the neutron $N = 82$ shell gap. The level spectra, up to 5 MeV of excitation in ^{131}In , ^{131}Sn , ^{130}In , ^{130}Cd , and ^{130}Sn , are well described and clearly explained by couplings of single-hole orbitals and by core excitations.

DOI: [10.1103/PhysRevC.88.054310](https://doi.org/10.1103/PhysRevC.88.054310)

PACS number(s): 21.10.-k, 21.60.Cs, 21.30.Fe, 27.60.+j

I. INTRODUCTION

Investigation of shell-structure changes in the neutron-rich region (e.g., for possible new magic numbers, the shell evolution as the neutron number varies, etc.) is at the forefront of nuclear physics research [1]. Nuclei with a few valence particles or valence holes close to a doubly closed shell are of particular importance for understanding the structure changes and for testing nuclear models. Recently, the magic nature of ^{132}Sn has been reconfirmed through a direct observation of single-particle states in its neighboring odd-mass isotopes [2,3]. On the other hand, studies of core-excited states probe correlations below and above the shell gaps and provide useful information on sizes of the gaps. For example, prompt and delayed γ -ray cascades in ^{131}Sn were studied at Gammasphere using a ^{248}Cm fission source which enabled one to obtain high-spin states in the energy range 4–5 MeV [4], supplying us with important information on the cross-shell excitations in this nucleus. A high-spin, core-excited isomer with $T_{1/2} = 630(60)$ ns in ^{131}In was identified following production by both relativistic fragmentation of a ^{136}Xe beam and fission of a ^{238}U beam, which provides a direct measure of the size of the neutron $N = 82$ shell gap [5].

Apart from its intrinsic importance for nuclear structure as mentioned above, the region around ^{132}Sn is also of astrophysical interest for understanding the formation of the $A \approx 130$ peak of the solar r -process (i.e., the rapid neutron-capture process) abundance distribution. It has been believed that the origin of nearly half of the solar abundances of elements heavier than the Fe group is the astrophysical r -process [6]. The early identification of the classical $N = 82$ r -process waiting-point isotope ^{130}Cd established such a connection to the nuclear structure problem [7]. Although the basic recipe for generating r -process elements is known, the detailed

production of heavy nuclei through repetitions of neutron capture and β decay remains to be understood. Considering the close relation between the $N = 82$ shell closure and the $A \approx 130$ peak of the solar r -process abundance distribution, the $N = 82$ isotones below the doubly magic nucleus ^{132}Sn are crucial for stellar nucleosynthesis [8]. The r -process reaction rates may be strongly impacted by the properties of neutron single particle states in this region [9]. It has been shown [10] that the impact of neutron capture rates near the $A = 130$ peak can alter the abundances of individual nuclear species throughout the abundance pattern. Very recent studies [11] have particularly investigated how the level structures in $^{131,133}\text{Sn}$ can influence the results of neutron capture cross sections that are relevant to r -process nucleosynthesis studies. The study [11] tried to connect the r -process predictions to the nuclear level measurements [2,9], and suggested the necessity for detailed experimental measurements of level structures of heavy neutron-rich nuclei that are in and near the r -process.

In addition, understanding isomeric states in these nuclei is also an important subject for both nuclear structure and nucleosynthesis studies [12]. Isomeric states are found to be abundant around the doubly magic ^{132}Sn , particularly in the isotopes a few holes away from ^{132}Sn [13,14]. They are typically formed by the so-called yrast spin traps [15]. The unique-parity $h_{11/2}$ neutron-hole orbital, which is found close to the Fermi levels for these nuclei, is responsible for the formation of this type of isomerism. Experimentally, many isomers have been identified and their structures discussed. For example, microsecond isomers in the In and Cd isotopes (the mass range $A = 123$ to 130) were investigated through thermal-neutron-induced fission reactions [16]. The total decay energies of two isomers in ^{131}Sn and the isomer decays in ^{131}In were also investigated [17]. An 8^+ two-quasiparticle isomer in the waiting-point nucleus ^{130}Cd was observed both in the fragmentation of a ^{136}Xe beam and the projectile fission of ^{238}U [8].

With a rich collection of recent experimental data, it is interesting to perform systematical shell-model calculations

* Corresponding author: sunyang@sjtu.edu.cn

that can consistently describe both low-lying and high-energy states for all kinds of (even-even, odd-mass, and odd-odd) nuclei near ^{132}Sn . Such shell model calculations may further be used to provide theoretical rates for neutron-capture and β decay for the nuclear astrophysics interest. In the past, various shell model calculations were applied to the ^{132}Sn mass region and contributed greatly to the structure analysis (see, for example, Refs. [4,5,8,16,18]). In a recent work [19], by employing the extended pairing-plus-quadrupole Hamiltonian combined with monopole corrections, the EPQQM model [20] has been applied to the ^{132}Sn region. It has been demonstrated that the model can provide a systematical description for energy levels of $A = 133\text{--}135$ nuclei up to high spins. The structure of these nuclei was analyzed in detail by the EPQQM model, with emphasis of effects associated with core excitations.

The aim of the present work is to apply the EPQQM model to investigate structures of the hole nuclei below the doubly closed shell, having one or two protons and/or neutrons less than ^{132}Sn . The article is arranged as follows. In Sec. II, we outline the EPQQM model and present the model space, the single-particle energies, and the parameters in the EPQQM interaction for the nuclei under consideration. In Sec. III, we discuss the calculated results of $A = 131$ and 130 nuclei, by showing detailed comparisons with available experimental data and with other previous theoretical calculations. Finally, conclusions are drawn in Sec. IV.

II. THE EPQQM MODEL

Shell model is the most fundamental method for nuclear structure analysis. It has been shown that a realistic shell-model Hamiltonian can be separated into the monopole and multipole parts [21,22]. The use of the separable forces in the nuclear Hamiltonian has advantages due to its simplicity. The application of the pairing and quadrupole interactions has a long history in the nuclear structure study [23–25], which considers the two most important excitation modes in nuclei. A successful example is the EPQQM model [20] employed in the present work. We note, in particular, that to compare with other models with effective forces, the EPQQM model requires much less parameters to determine the interaction. It has been demonstrated that despite its simplicity, the EPQQM model works surprisingly well for different mass regions, for example, the proton-rich pf shell [26] and the $pf_{5/2}g_{9/2}$ shell [27], the neutron-rich fp_g shell [28], and the sd - pf shell region [29]. Next, we present the Hamiltonian, the employed model space, and the parameters including the single-particle states.

A. The Hamiltonian

With protons and neutrons occupying different shells, the Hamiltonian, which consists of the pairing-plus-multipole force and the monopole corrections, is given by the following proton-neutron (pn) representation:

$$\begin{aligned} H &= H_{\text{sp}} + H_{P_0} + H_{P_2} + H_{Q_0} + H_{O_0} + H_{HH} + H_{\text{mc}} \\ &= \sum_{\alpha,i} \varepsilon_a^i c_{\alpha,i}^\dagger c_{\alpha,i} - \frac{1}{2} \sum_{J=0,2} \sum_{ii'} g_{J,ii'} \sum_M P_{JM,ii'}^\dagger P_{JM,ii'} \end{aligned}$$

TABLE I. The two-body force strengths (in MeV).

ii'	$g_{0,ii'}$	$g_{2,ii'}$	$\chi_{2,ii'}$	$\chi_{3,ii'}$	$\chi_{4,ii'}$
pp	0.250	0.158	0.102	0.032	0.0014
nn	0.129	0.047	0.140	0.004	0.0008
pn	0	0	0.082	0	0.0009

$$\begin{aligned} & - \frac{1}{2} \sum_{ii'} \frac{\chi_{2,ii'}}{b^4} \sum_M : Q_{2M,ii'}^\dagger Q_{2M,ii'} : \\ & - \frac{1}{2} \sum_{ii'} \frac{\chi_{3,ii'}}{b^6} \sum_M : O_{3M,ii'}^\dagger O_{3M,ii'} : \\ & - \frac{1}{2} \sum_{ii'} \frac{\chi_{4,ii'}}{b^8} \sum_M : H_{4M,ii'}^\dagger H_{4M,ii'} : \\ & + \sum_{a \leq b, ii'} k_{\text{mc}}(ia, i'b) \sum_{JM} A_{JM}^\dagger(ia, i'b) A_{JM}(ia, i'b). \end{aligned} \quad (1)$$

In Eq. (1), the single-particle Hamiltonian (H_{sp}), the $J = 0$ and $J = 2$ pairing ($P_0^\dagger P_0$ and $P_2^\dagger P_2$), the quadrupole-quadrupole ($Q^\dagger Q$), the octupole-octupole ($O^\dagger O$), the hexadecapole-hexadecapole ($H^\dagger H$) terms, and the monopole corrections (H_{mc}) are included. In the pn representation, $P_{JM,ii'}^\dagger$ and $A_{JM}^\dagger(ia, i'b)$ are the pair operators, and $Q_{2M,ii'}^\dagger$, $O_{3M,ii'}^\dagger$, and $H_{4M,ii'}^\dagger$ are the quadrupole, octupole, and hexadecapole operators, respectively, in which i and i' are indices for proton or neutron. The constants $g_{J,ii'}$, $\chi_{2,ii'}$, $\chi_{3,ii'}$, $\chi_{4,ii'}$, and $k_{\text{mc}}(ia, i'b)$ are the corresponding force strengths, and b is the harmonic-oscillator range parameter. The force strengths determined for the present calculation are listed in Table I.

B. The model space and parameters

Our model space for the present study includes five neutron levels below the neutron magic number $N = 82$ ($0g_{7/2}$, $1d_{5/2}$, $2s_{1/2}$, $0h_{11/2}$, $1d_{3/2}$) and four proton levels below the proton magic number $N = 50$ ($0f_{5/2}$, $1p_{3/2}$, $1p_{1/2}$, $0g_{9/2}$). That means that the closed core is ^{78}Ni . To describe neutron core-excited states, we add in our model space another two neutron orbits ($1f_{7/2}$, $2p_{3/2}$) above the neutron $N = 82$ shell gap to allow core excitations. In addition, we include two proton orbits ($0g_{7/2}$, $1d_{5/2}$) above the proton $N = 50$ shell gap, which were also included in Ref. [5]. Thus the chosen model space is large, which emphasizes a full description of the low-lying states, including those dominated by the proton $\pi f_{5/2}$ and $\pi p_{3/2}$ single-particle states. In fact, there have been experimental evidences that considerably large $\log(ft)$ value of Gamow-Teller decay from ^{131}Cd to the low-lying $5/2^-$ state in ^{131}In was obtained [30].

The low-lying states in ^{131}In are taken as the proton single particle states in our model space, and those in ^{131}Sn and ^{133}Sn as the neutron single-particle states. Writing ε_a^i as the single-particle energy, with i being π or ν and a denoting an orbital, we have, for example,

$$\varepsilon_{g_{9/2}}^\pi = BE(^{131}\text{In}) - BE(^{132}\text{Sn}) = -15.690 \text{ MeV}, \quad (2)$$

where $BE(X)$ in Eq. (2) is the negative total binding energy of a nucleus X . For other proton single particle energies, we simply consider the known experimental information, for example,

$$\varepsilon_{p1/2}^{\pi} = \varepsilon_{g9/2}^{\pi} - 0.302 \text{ MeV} = -15.992 \text{ MeV}, \quad (3)$$

in which 0.302 MeV is taken from the experimental energy of the lowest $1/2^-$ state in ^{131}In . Similarly, we get all other proton and neutron single-particle energies as shown below (all in MeV):

$$\begin{aligned} \varepsilon_{f5/2}^{\pi} &= -18.440, & \varepsilon_{p3/2}^{\pi} &= -17.340, \\ \varepsilon_{p1/2}^{\pi} &= -15.992, & \varepsilon_{g9/2}^{\pi} &= -15.690, \\ \varepsilon_{g7/2}^{\pi} &= -9.677, & \varepsilon_{d5/2}^{\pi} &= -8.715, \\ \varepsilon_{g7/2}^{\nu} &= -9.788, & \varepsilon_{d5/2}^{\nu} &= -9.009, \\ \varepsilon_{s1/2}^{\nu} &= -7.686, & \varepsilon_{h11/2}^{\nu} &= -7.422, \\ \varepsilon_{d3/2}^{\nu} &= -7.354, & \varepsilon_{f7/2}^{\nu} &= -2.372, \\ \varepsilon_{p3/2}^{\nu} &= -1.518. \end{aligned}$$

It can be seen that the energy difference for the single-particle levels across the neutron $N = 82$ shell gap is $\varepsilon_{f7/2}^{\nu} - \varepsilon_{d3/2}^{\nu} = 4.982$ MeV, while that across the proton $N = 50$ shell gap is $\varepsilon_{g7/2}^{\pi} - \varepsilon_{g9/2}^{\pi} = 6.013$ MeV. These values correspond well with the choice of 5 MeV for the neutron $N = 82$ shell gap [4] and 6 MeV for the proton $N = 50$ gap [30], respectively. If we take ^{78}Ni as the core, the energy differences between the hole and particle states should be considered to modify the energy levels below ^{132}Sn [19]. For the truncated model space, the monopole terms should also be considered to compensate partly for the truncation. The monopole migration is one of the two main mechanisms that are predicted to drive the possible shell evolution phenomena [1]. Two monopole corrections, $M1 \equiv k_{\text{mc}}(\nu h_{11/2}, \nu f_{7/2}) = 0.52$ MeV and $M2 \equiv k_{\text{mc}}(\pi g_{9/2}, \nu h_{11/2}) = -0.40$ MeV, are employed in the present calculation. The $M1$ term, for example, can sensitively influence the results when neutron core excitations are involved. Their detailed effects will be discussed later. In the calculation, we allow only one proton and one neutron to be excited from the core.

III. RESULTS AND DISCUSSIONS

We use the shell model code NUSHELLX [31] for calculation. The magic character of ^{132}Sn has been demonstrated by the recent experiments, in the high-precision direct Penning trap mass measurement for $^{132,134}\text{Sn}$ [32], and the measurement of energy spectrum of ^{133}Sn [2] that has one valence neutron outside ^{132}Sn . The relatively simple structure of near doubly closed-shell nuclei is recognized in their observed spectra which are usually understood as consisting of two types of excitations: excitations of valence single particles (or holes) and excited states formed by couplings of the valence nucleons to core excitations. The most important core excitation for the nuclei under consideration is the one in which an $h_{11/2}$ neutron is excited across the $N = 82$ shell gap to the $f_{7/2}$ level, forming essentially a $\nu h_{11/2}^{-1} f_{7/2}$ structure.

In the following, five-hole nuclei below ^{132}Sn are studied. These are the 1π -hole nucleus ^{131}In , the 1ν -hole ^{131}Sn , the

1π - 1ν -hole ^{130}In , the 2π -hole nucleus ^{130}Cd , and the 2ν -hole ^{130}Sn .

A. ^{131}In

The nucleus ^{131}In has one proton-hole relative to ^{132}Sn . The four low-lying states in this nucleus, i.e., the positive-parity ground state $9/2^+$ and the three lowest negative-parity states $1/2^-$, $3/2^-$, and $5/2^-$, are mainly the proton single-hole states. The high-energy states in ^{131}In involve cross-shell excitations. In an early work [33], two β -emitting isomers in ^{131}In were identified above the $9/2^+$ ground state with the proposed spin-parity $1/2^-$ and $21/2^+$, respectively. Among them, the 350(50) ms isomeric state $1/2^-$ lies just above the ground state at the excitation 0.302 MeV [17]. The 320(60) ms high-spin isomer $21/2^+$ observed at 3.764 MeV has a structure with neutron core excitation. The excitation energy of this state provides a direct measure of the size of the $N = 82$ shell gap, which was considered as an important piece of structure information for this mass region [5].

Figure 1 shows the results of the present shell-model calculation for ^{131}In , which is compared with the available experimental data. Besides of the four proton single-hole states, our calculation can well reproduce the two known core-excitation states $21/2^+$ and $17/2^+$. The calculation further suggests that two more states ($23/2^+$ and $25/2^+$) are almost degenerate with the $21/2^+$ state, and a $19/2^+$ state

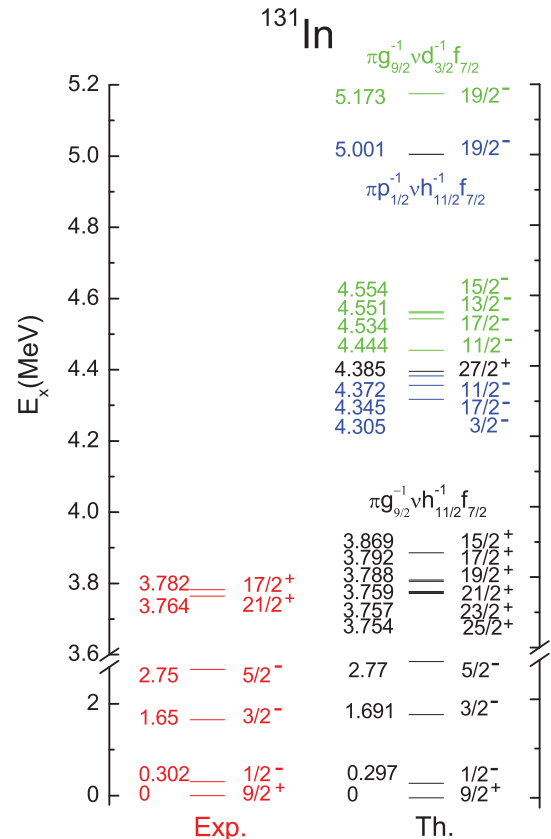


FIG. 1. (Color online) The experimental energy levels in ^{131}In taken from [36] and the results of shell-model calculation.

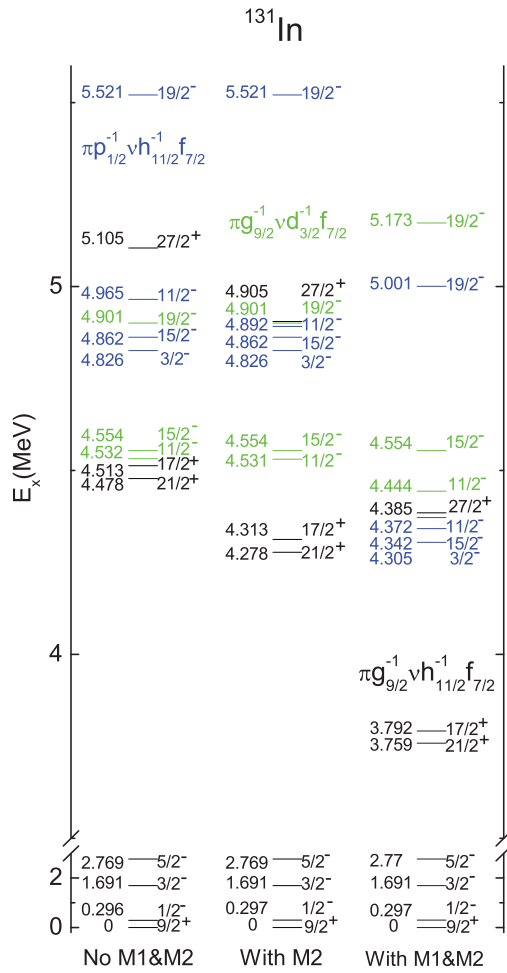


FIG. 2. (Color online) Effects of the proposed monopole corrections in the ^{131}In calculation.

lies very close to $17/2^+$. In this nucleus, the states involving cross-shell excitations are those in which an $h_{11/2}$ neutron below the $N = 82$ shell gap is excited to occupy the upper levels above the gap. According to our calculation, the most favorite configuration of such is $\pi g_{9/2}^{-1} \nu h_{11/2}^{-1} f_{7/2}$, in agreement with the result in Ref. [5]. In the present calculation, both of the employed monopole terms $M1$ and $M2$ contribute to lower the $17/2^+$ and $21/2^+$ states to reproduce the experimental data. Thus, it is important to recognize that these two monopole corrections help to realize the size of the neutron $N = 82$ shell gap in our model.

The effects of monopole correction in the ^{131}In calculation are illustrated in Fig. 2. If no monopole corrections are included in the calculation, the experimentally observed core-excited $21/2^+$ and $17/2^+$ states are too high at about 4.5 MeV, as shown in the leftmost column of the figure. The other core-excited states lie even higher in energy. The levels are pushed down considerably by the monopole terms. With the proposed monopole strengths, the experimentally known $21/2^+$ and $17/2^+$ levels can be correctly reproduced (see the rightmost column of Fig. 2 and compare it with Fig. 1). Comparing the results in the middle column with those in the rightmost column, we find that the monopole term $M1$ plays

more important role as it changes the levels significantly. It is also clear, from Fig. 2, that the amount shifted by the monopole corrections depends on configurations. It can be seen that the maximal effect occurs for the configuration $\pi g_{9/2}^{-1} \nu h_{11/2}^{-1} f_{7/2}$, which feels both of the $M1$ and $M2$ corrections. We have thus provided a clear evidence of the monopole effect for high energy regions.

Having fixed the neutron shell gap through interactions, we can make predictions for other core-excited states that have not been observed. Concerning the negative-parity levels, the calculation of Górska *et al.* [5] suggested that the lowest one is an $11/2^-$ state with the configuration $\pi g_{9/2}^{-1} \nu d_{3/2}^{-1} f_{7/2}$. As can be seen in Fig. 1, our calculation, however, predicts that the negative-parity configuration $\pi p_{1/2}^{-1} \nu h_{11/2}^{-1} f_{7/2}$ lies lower in energy than the $\pi g_{9/2}^{-1} \nu d_{3/2}^{-1} f_{7/2}$ one. It seems that our suggested configuration is a natural consequence of the coupling of the lowest-excited proton-hole $\pi p_{1/2}$ state to the neutron $\nu h_{11/2}^{-1} f_{7/2}$ particle-hole excitation. At some higher excitation energies starting from 4.444 MeV, the negative-parity configuration $\pi g_{9/2}^{-1} \nu d_{3/2}^{-1} f_{7/2}$ is predicted to appear also in our calculation, with the lowest state in this configuration being $11/2^-$. To resolve the difference in predictions between the two shell models, ours and that of Ref. [5], g factor measurements for this mass region [34,35] would be helpful, which may distinguish the single-particle structure in the two suggested configurations in ^{131}In associated with the lowest core-excited negative-parity states.

B. ^{131}Sn

With one neutron less than ^{132}Sn , ^{131}Sn is an important nucleus to study neutron single-hole states and associated core excitations, and therefore, has attracted a lot of attention during the years [4,9,17]. After we have determined the necessary monopole correction terms for studying neutron cross-shell excitations in ^{131}In , as discussed in the last subsection, calculation for ^{131}Sn can be another important test for the interactions determined in the EPQQM model.

The ^{131}Sn ground state is believed to be $3/2^+$ and the first excited state is the $1h_{11/2}$ hole state at about 65 keV excitation [36]. Above them there are known neutron single-hole states $1/2^+$ at 0.332 MeV, $5/2^+$ at 1.655 MeV, and $7/2^+$ at 2.434 MeV, which were tentatively determined from β -decay experiments [37].

Prompt and delayed γ -ray cascades in ^{131}Sn were studied by Bhattacharyya *et al.* [4] at Gammasphere using a ^{248}Cm fission source which enabled them to obtain high-spin states in the energy range 4–5 MeV. Their experimental results were interpreted with the shell model using empirical nucleon-nucleon interactions [4]. Our present shell-model calculation with the EPQQM Hamiltonian supports their interpretation for the high-spin states. The results are given in Fig. 3 and the high spin part is plotted in Fig. 4 for clarity.

The configuration for the experimentally observed positive-parity states $21/2^+$, $19/2^+$, $17/2^+$, and $15/2^+$ is interpreted in our calculation as $\nu h_{11/2}^{-1} d_{3/2}^{-1} f_{7/2}$, which agrees with the conclusion in Ref. [4]. As can be seen in the left part of Fig. 4, the theoretical $21/2^+$ level at 4.859 MeV is very close to the experimental one at 4.99 MeV, and the theoretical $17/2^+$

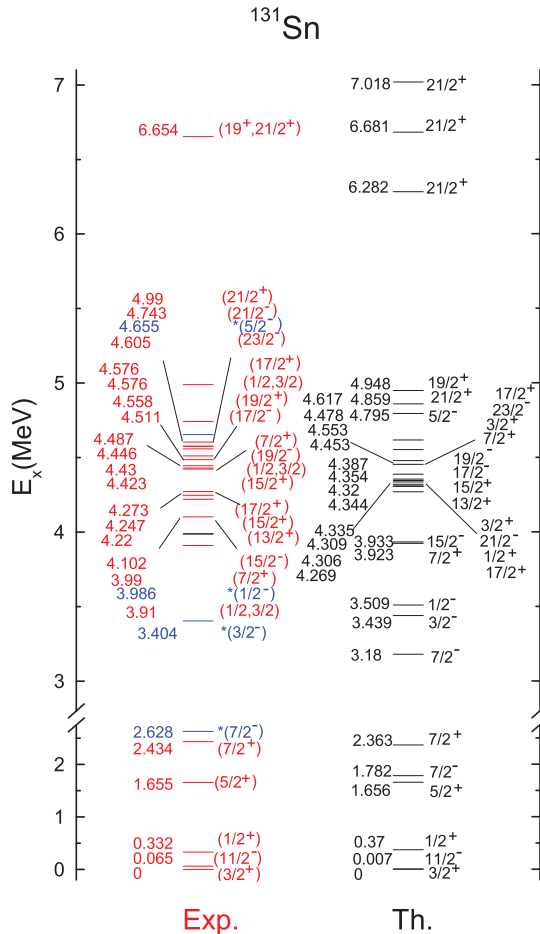


FIG. 3. (Color online) The experimental energy levels in ^{131}Sn taken from [36] and the results of shell model calculation. The four experimental levels (blue color marked with star) are the latest experimental energy levels [9].

level at 4.269 MeV fits the experimental one at 4.273 MeV perfectly. Also in agreement with the previous shell model interpretations [4,17], the negative-parity sequence with the multiplet of $15/2^-$, $17/2^-$, $19/2^-$, $21/2^-$, $23/2^-$ are found to belong to the configuration $\nu h_{11/2}^{-2} f_{7/2}$, and their energies are also well reproduced by our calculation. As can be seen in the right part of Fig. 4, our calculated energy level $15/2^-$ at 3.933 MeV fits the experimental isomeric state at 4.102 MeV, and the calculated $23/2^-$ at 4.478 MeV agrees the

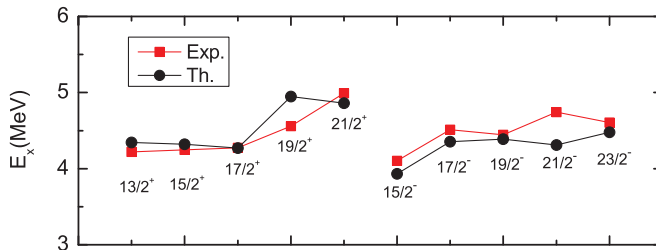


FIG. 4. (Color online) Comparison of the high-spin part of the calculated energy levels (black dots) with experimental data [4] (red squares) in ^{131}Sn .

experimental one at 4.605 MeV. Once again, all these have provided a strong support to our treatment for the neutron $h_{11/2}^{-1} f_{7/2}$ core excitation.

Also in the energy range of 4–5 MeV, the calculated energy values for the two $7/2^+$ states (3.923 and 4.453 MeV) are found to be very close to the experimental data at 3.99 and 4.487 MeV. An early experiment for ^{131}In β decay [33] determined a ^{131}Sn level at 6.654 MeV with $(\nu g_{7/2}^{-1} h_{11/2}^{-1} f_{7/2})$ and tentatively assigned it as $21/2^+$. Our present calculation reveals three $21/2^+$ core-excited states in this energy range. The one at 6.681 MeV is of the configuration $\nu d_{5/2}^{-1} h_{11/2}^{-1} f_{7/2}$. The other two have the configuration $\nu g_{7/2}^{-1} h_{11/2}^{-1} f_{7/2}$, lying at 6.282 MeV and 7.018 MeV, respectively.

In a very recent work reported in Ref. [9], Kozub *et al.* performed a $^{130}\text{Sn}(d, p)^{131}\text{Sn}$ reaction and compared their results with those of the $^{132}\text{Sn}(d, p)^{133}\text{Sn}$ one [2]. They suggested, based on the similar results from both reactions, that their observed four new states in ^{131}Sn , ranging roughly from 2.6 to 4.7 MeV, are mainly the neutron single-particle states above the $N = 82$ shell gap. These four experimental states are included in Fig. 3 (those marked with stars). The work of Ref. [9] actually suggested that the observed states in ^{131}Sn have a structure of a pair of neutron hole states (2h) coupled to one neutron particle (1p), forming a 2h-1p structure. While the 2h states can be one of $\nu h_{11/2}^{-2}$, $\nu d_{3/2}^{-2}$, and $\nu h_{11/2}^{-1} d_{3/2}^{-1}$, or a combination of them, the 1p state must be relatively pure, being from one of the $\nu f_{7/2}$, $\nu p_{3/2}$, $\nu p_{1/2}$, and $\nu f_{5/2}$ orbital above the neutron $N = 82$ gap.

A state at the 2.628-MeV excitation was tentatively signed as $7/2^-$ in Ref. [9]. Our shell-model calculation yields two $7/2^-$ states in the low-energy region, at 1.782 MeV and 3.18 MeV. Both of the calculated states have a large component (75–80 %) from $\nu h_{11/2}^{-2} f_{7/2}$, consistent with the anticipated configuration of Ref. [9] for this state. It is seen that the two theoretical $7/2^-$ states share the same major component as the multiplet states (from $13/2^-$ to $23/2^-$) as shown in the right part of Fig. 4. Another experimental state at 3.404 MeV excitation in ^{131}Sn was tentatively signed as $3/2^-$ [9], which was expected to be mainly of the $\nu(2h)p_{3/2}$ structure. Our calculation gives a $3/2^-$ state lying at 3.439 MeV excitation. However, it is mainly of the structure $\nu(2h)f_{7/2}$. We note that fragmentation in configurations is normally expected in shell-model states of high excitation. The current model space may still be too small to talk about the experimental levels marked with stars in Fig. 3. The truncation would affect the position for the calculated $7/2^-$ levels. Finally, our model space does not include the neutron particle orbital $p_{1/2}$ and $f_{5/2}$ above the $N = 82$ shell gap, and therefore, we can not say anything about the experimental states reported for $(1/2^-, 3.986 \text{ MeV})$ and $(5/2^-, 4.655 \text{ MeV})$ in Ref. [9].

C. ^{130}In

The nucleus ^{130}In is an odd-odd system, which has one proton- and one neutron-hole with regard to ^{132}Sn . It is an ideal case to probe the correlations between the proton- and neutron-hole states, as well as the interplay with core-excitations. The low-lying configurations in ^{130}In are expected to be formed by couplings of the proton and neutron single-hole states as

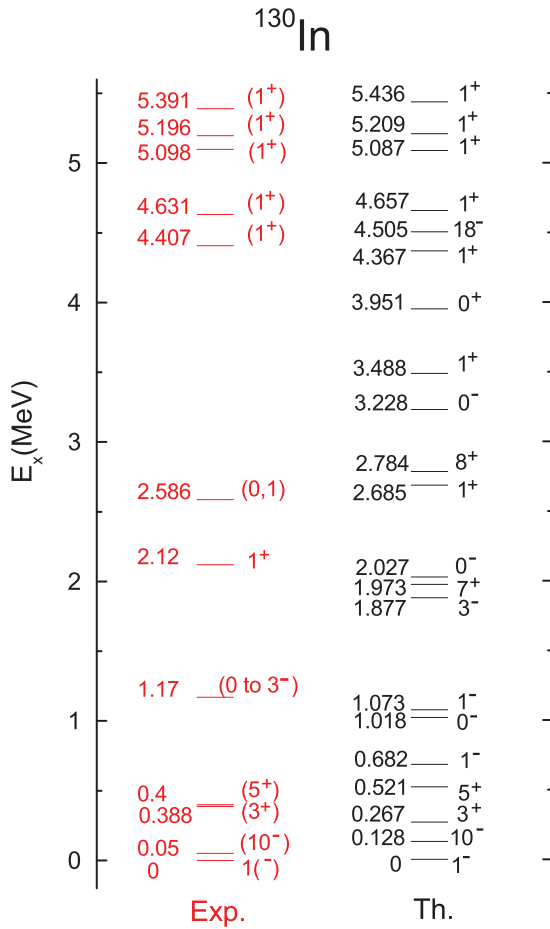


FIG. 5. (Color online) The experimental energy levels in ^{130}In taken from [36] and the results of the shell-model calculation.

those appearing in ^{131}In and ^{131}Sn . Fig. 5 shows the calculated results for ^{130}In . The shell-model calculation predicts that the dominant component for the ground state configuration in ^{130}In is $\pi g_{9/2}^{-1} \nu h_{11/2}^{-1}$, for which the multiplet consists of ten states from 1^- to 10^- . The calculated states belonging to this configuration are shown in Fig. 6. The experimentally known 10^- state lies at 50 keV above the 1^- ground state. Our calculation yields the 10^- state at 128 keV.

At the 0.682-MeV excitation, we predict another 1^- state built by $\pi p_{1/2}^{-1} \nu d_{3/2}^{-1}$, to which there are currently no data to correspond. Near the excitation of 400 keV, there are two experimentally-known positive-parity states, tentatively

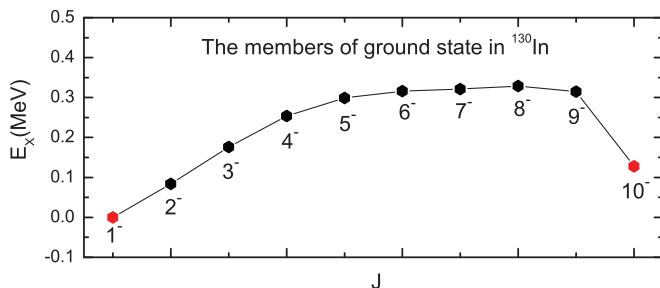


FIG. 6. (Color online) The members of the $\pi g_{9/2}^{-1} \nu h_{11/2}^{-1}$ multiplet predicted by the shell-model calculation for ^{130}In .

assigned as 3^+ and 5^+ . As one can see from Fig. 5, our calculation gives a fairly good reproduction for these two states. The calculation shows that the major configuration for the 3^+ and 5^+ states is $\pi g_{9/2}^{-1} \nu d_{3/2}^{-1}$, in agreement with the previous shell-model predictions [17,38]. All the above-discussed states are the consequences of couplings of the lowest neutron-hole and proton-hole states.

In Fig. 5, there is an experimental level at 1.17 MeV with uncertainty in spin-parity and marked as $(0 \text{ to } 3^-)$. From the calculation, we find several negative-parity states in the same energy range. For example, our calculation suggests another 1^- state at 1.073 MeV with the configuration $\pi p_{1/2}^{-1} \nu d_{3/2}^{-1}$, sharing the same configuration with the first 0^- state at 1.018 MeV. The second 0^- state at 2.027 MeV has mainly the configuration $\pi p_{3/2}^{-1} \nu d_{3/2}^{-1}$. In addition, a 3^- state at 1.877 MeV is predicted to have a very pure configuration $\pi p_{3/2}^{-1} \nu h_{11/2}^{-2} f_{7/2}$, which is the lowest core-excited state in this nucleus.

Among the higher-spin states with couplings of one-proton hole and one-neutron hole in ^{130}In , we predict a 7^+ state at 1.973 MeV having the configuration $\pi g_{9/2}^{-1} \nu d_{5/2}^{-1}$ and an 8^+ state at 2.784 MeV having the configuration $\pi g_{9/2}^{-1} \nu g_{7/2}^{-1}$ (see Fig. 5).

For the $N = 82$ waiting-point nuclides, the relevant nuclear-structure properties are the Q value and the location of the $(\pi g_{9/2} \nu g_{7/2})$ configuration for the 1^+ level in ^{130}In populated by Gamow-Teller (GT) decay. These structure aspects for understanding of the r -process nucleosynthesis were extensively discussed by Dillmann *et al.* [38]. As an important discovery, they reported [38] the 1^+ level in ^{130}In at 2.12 MeV with the clean transitions from this state to the lower-lying states including the 1^- ground state. It was pointed out [38] that the position of this level is determined by the strength of the proton-neutron interaction between the spin-orbit partners $\pi g_{9/2}$ and $\nu g_{7/2}$ relative to the $\pi g_{9/2}$ and $\nu h_{11/2}$ orbitals, as well as the difference between the position of the $h_{11/2}$ and the $g_{7/2}$ orbitals. In their calculation [38], Dillmann *et al.* obtained an energy 1.38 MeV for this level. The large-scale shell-model calculation by Martinez-Pinedo and Langanke [39] predicted this 1^+ level at 1.555 MeV. The present calculation yields the lowest 1^+ state at 2.685 MeV having the $\pi g_{9/2}^{-1} \nu g_{7/2}^{-1}$ structure, which reproduces the data much better. In addition to this 1^+ state, several other experimental data of 1^+ states are available [36]. In Table II, we list also those data together

TABLE II. The predicted 1^+ levels in ^{130}In with their main configurations. Available experimental data are displayed for comparison.

	Exp.	Th.	Conf.
1^+	2.12	2.685	$\pi g_{9/2}^{-1} \nu g_{7/2}^{-1}$
(1^+)		3.488	$\pi p_{1/2}^{-1} \nu h_{11/2}^{-2} f_{7/2}$
(1^+)	4.407	4.367	$\pi p_{1/2}^{-1} \nu h_{11/2}^{-2} f_{7/2}$
(1^+)	4.63	4.657	$\pi p_{1/2}^{-1} \nu h_{11/2}^{-2} f_{7/2}$
(1^+)	5.098	5.087	$\pi p_{1/2}^{-1} \nu h_{11/2}^{-2} f_{7/2}$
(1^+)	5.196	5.209	$\pi g_{9/2}^{-1} \nu d_{3/2}^{-1} h_{11/2}^{-1} f_{7/2}$
(1^+)	5.391	5.436	$\pi g_{9/2}^{-1} \nu d_{3/2}^{-1} h_{11/2}^{-1} f_{7/2}$

with our shell-model predictions. All these high-energy 1^+ states belong to configurations with core excitation.

Levels with core excitation in ^{130}In are expected in the energy range higher than 3 MeV excitation. For example, the calculation predicts the core-excited state at 3.228 MeV, with spin-parity 0^- and configuration $\pi g_{9/2}^{-1} \nu h_{11/2}^{-2} f_{7/2}$. The predicted 0^+ state at 3.951 MeV is another core-excited state with $\pi g_{9/2}^{-1} \nu h_{11/2}^{-1} d_{3/2}^{-1} f_{7/2}$. A high-spin 18^- state at 4.505 MeV appears in the calculation with a very pure configuration $\pi g_{9/2}^{-1} \nu h_{11/2}^{-2} f_{7/2}$, and could be a good high-spin isomer.

D. ^{130}Cd

^{130}Cd is the classical $N = 82$ r -process waiting-point isotope, first identified by Kratz *et al.* in 1986 [7], for which a β -decay half-life of $T_{1/2} = (195 \pm 35)$ ms could be determined from multi-scaling of β -delayed neutrons. In Ref. [8], Jungclaus *et al.* observed a γ decay of excited states in this nucleus, with an 8^+ isomer populated both in the fragmentation of a ^{136}Xe beam as well as in the projectile fission of ^{238}U .

Our shell-model calculation confirms that the configuration of the low-lying positive-parity states $0^+, 2^+, 4^+, 6^+, 8^+$ in ^{130}Cd is mainly of the $\pi g_{9/2}^{-2}$ configuration. Our calculation predicts the lowest negative-parity states 5^- and 4^- in ^{130}Cd at about 2.37 MeV, consistent with the results of Jungclaus *et al.* [8]. The corresponding negative-parity configuration is of the proton two-hole nature, namely $\pi g_{9/2}^{-1} p_{1/2}^{-1}$. Our results also suggest a 3^- state at 3.631 MeV with the proton two-hole configuration $\pi g_{9/2}^{-1} p_{3/2}^{-1}$. These configurations are expected in a sense of simple shell-model couplings for the proton two-hole states.

No experiment regarding states with core excitation has been reported for this nucleus. The shell-model calculation in Ref. [8] could not deal with neutron core-excitations due to their limited model spaces. As shown in Fig. 7, the lowest neutron core-excited state in ^{130}Cd is predicted by our calculation to be 7^+ at 3.705 MeV, with the configuration $\pi g_{9/2}^{-2} \nu h_{11/2}^{-1} f_{7/2}$.

E. ^{130}Sn

^{130}Sn is the daughter nucleus to which ^{130}In β decays. At least three lowest-lying states in ^{130}In are known to decay to ^{130}Sn : the 1^- ground state, the 10^- state at 50 keV, and the 5^+ state at 400 keV. To describe the decay rates, it is desired to establish a shell model framework that can describe these level structures of the β -decay parent and daughter nuclei consistently.

According to our calculation, the 0^+ ground state in ^{130}Sn has a mixed structure, with about half of the $\nu(h_{11/2})^{-2}$ configuration and some $\nu(d_{3/2})^{-2}$. The calculation suggests that the yrast states $2^+, 4^+, 6^+, 8^+, 10^+$ (see Fig. 8) belong to the multiplet of $\nu(h_{11/2})^{-2}$. The predicted second 2^+ state at 1.811 MeV, which has a very mixed structure [$\nu(d_{3/2})^{-2}$, $\nu(s_{1/2})^{-1}(d_{3/2})^{-1}$, etc.], may be compared with the experimental (2^+) state at 2.028 MeV.

In Fig. 8, the observed 7^- level at 1.947 MeV is a well-known isomeric state [14], with a 1.7(1) min half-life. In

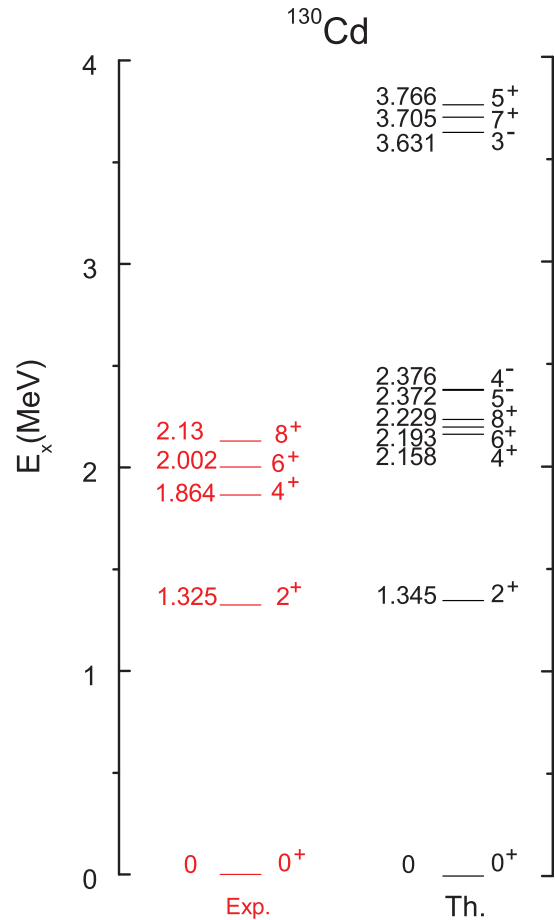


FIG. 7. (Color online) The experimental energy levels in ^{130}Cd taken from [36] and the results of the shell-model calculation.

agreement with the previous conclusions, our result suggests that this state belongs to the $\nu(d_{3/2})^{-1}(h_{11/2})^{-1}$ quartet together with the $6^-, 5^-$, and 4^- states. Our calculation obtains the energy for the 7^- level at 2.023 MeV, in a perfect agreement with experiment. However, we predict that the 4^- state from the quartet lies below $5^-, 6^-$, and 7^- , which disagrees with the tentative order for the states from experiment. Nevertheless, this should not affect the isomeric nature of the 7^- state because of the unfavored $M3$ transition between this and the 4^- state. We predict a 6^- state from this quartet at 2.242 MeV, which has not been observed.

Our calculation suggests a 3^- state at 3.335 MeV [$\nu(d_{5/2})^{-1}(h_{11/2})^{-1}$] and a 4^+ state at 3.515 MeV [$\nu(d_{5/2})^{-1}(d_{3/2})^{-1}$], which may be compared with the experimental 3.167-MeV and 3.425-MeV level, respectively. The candidates for the experimental (2^-) level at 4.120 MeV, (9^-) at 4.206 MeV, ($3^-, 4^+$) at 4.225 MeV, (4^+) at 4.405 or 4.463 MeV would be, respectively, our calculated states at 3.922 MeV [$\nu(g_{7/2})^{-1}(h_{11/2})^{-1}$], 4.335 MeV [$\nu(g_{7/2})^{-1}(h_{11/2})^{-1}$], 4.288 MeV [$\nu(g_{7/2})^{-1}(h_{11/2})^{-1}$], and 4.528 MeV [$\nu(g_{7/2})^{-1}(d_{3/2})^{-1}$].

The calculation for ^{130}Sn also yields states of core excitation, starting roughly from 4 MeV in excitation. The lowest one of such lies at 3.812 MeV, which is predicted as 3^- with the configuration $\nu(d_{3/2})^{-1}(h_{11/2})^{-2} f_{7/2}$. The theoretical

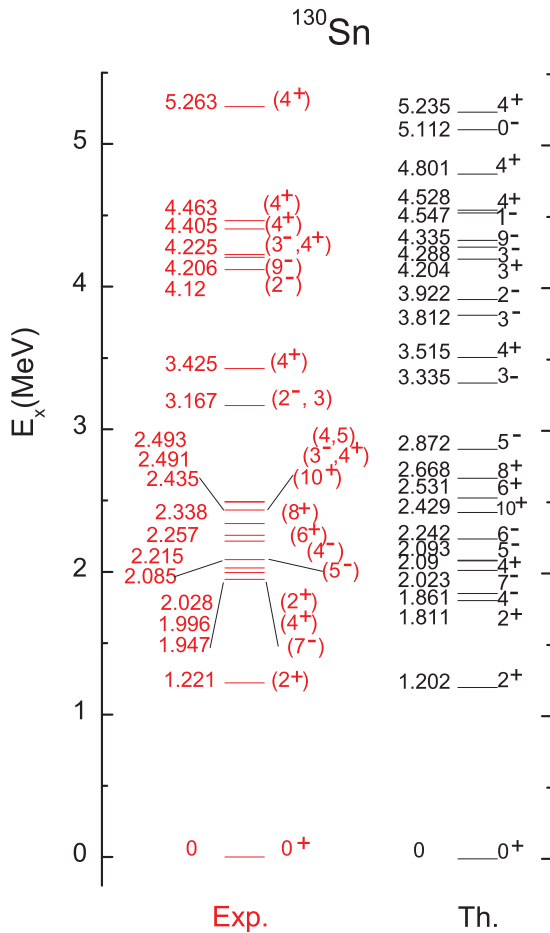


FIG. 8. (Color online) The experimental energy levels in ^{130}Sn taken from [36] and the results of the shell-model calculation.

4^+ state at 5.235 MeV has the configuration $\nu(h_{11/2})^{-3}f_{7/2}$, which fits the experimental level (4^+ , 5.263 MeV) very well. In addition, the calculation predicts the core-excited states of 1^- at 4.547 MeV and 0^- at 5.112 MeV with the common configuration $\nu d_{3/2}^{-1}h_{11/2}^{-2}f_{7/2}$.

IV. CONCLUSION

The study of neutron-rich nuclei near the doubly magic nucleus ^{132}Sn has been an important subject for nuclear structure and nuclear astrophysics research. One of the

challenging problems in shell-model calculations is to find out suitable effective interactions that work for the description of both low-lying states and core excitations. The theoretical development reported in this article is a sequential work of Ref. [19] that discussed neutron-rich nuclei beyond ^{132}Sn . These works are very relevant to the ongoing experimental programs in advanced facilities worldwide.

By means of large-scale shell-model calculations, we have carried out a structure study for the $A = 131$ and 130 hole nuclei near ^{132}Sn . The calculation considers both neutron and proton core-excitations across the shell gaps. The employment of the EPQQM model has made it possible to define the effective pp , nn , and pn interactions for a considerably large model space, which consists of seven neutron orbits ($0g_{7/2}$, $1d_{5/2}$, $2s_{1/2}$, $1d_{3/2}$, $0h_{11/2}$, $1f_{7/2}$, $2p_{3/2}$) and six proton orbits ($0f_{5/2}$, $1p_{3/2}$, $1p_{1/2}$, $0g_{9/2}$, $0g_{7/2}$, $1d_{5/2}$). With a set of determined parameters, the model has explained the experimental energy levels, not only the low-energy states but also those high-energy ones with core excitations in ^{131}In , ^{131}Sn , ^{130}In , ^{130}Cd , and ^{130}Sn . To best reproduce the data, we have introduced two monopole correction terms into the Hamiltonian, and their clear effects for the calculated spectrum have been demonstrated.

The present paper, together with the previous publication in Ref. [19], has shown the feasibility of the EPQQM model for explaining various nuclei near ^{132}Sn . The effective interaction with the separable forces derived from the EPQQM model has been proven to be capable of capturing the main physics of core excitations in this mass region. The predictions, in particular those high-energy states formed by core excitations, await future experimental confirmation. We are aware that the quality of our results relies heavily on the monopole corrections, which are phenomenological in nature. For a microscopic treatment, one should consider interactions including the monopole-based forces as recently suggested by Otsuka *et al.* [40].

ACKNOWLEDGMENTS

The authors are deeply grateful to Professor Munetake Hasegawa for sharing his knowledge and experience in shell-model calculations during his visit to Shanghai Jiao Tong University (SJTU). Research at SJTU was supported by the National Natural Science Foundation of China (Nos. 11075103 and 11135005) and by the 973 Program of China (No. 2013CB834401).

[1] T. Otsuka, T. Suzuki, R. Fujimoto, H. Grawe, and Y. Akaishi, *Phys. Rev. Lett.* **95**, 232502 (2005).
 [2] K. L. Jones *et al.*, *Nature (London)* **465**, 454 (2010).
 [3] K. L. Jones *et al.*, *Phys. Rev. C* **84**, 034601 (2011).
 [4] P. Bhattacharyya *et al.*, *Phys. Rev. Lett.* **87**, 062502 (2001).
 [5] M. Górska *et al.*, *Phys. Lett. B* **672**, 313 (2009).
 [6] M. E. Burbidge, G. R. Burbidge, W. A. Fowler, and F. Hoyle, *Rev. Mod. Phys.* **29**, 547 (1957).
 [7] K. L. Kratz *et al.*, *Z. Phys. A* **325**, 489 (1986).
 [8] A. Jungclaus *et al.*, *Phys. Rev. Lett.* **99**, 132501 (2007).

[9] R. L. Kozub *et al.*, *Phys. Rev. Lett.* **109**, 172501 (2012).
 [10] R. Surman, J. Beun, G. C. McLaughlin, and W. R. Hix, *Phys. Rev. C* **79**, 045809 (2009).
 [11] S.-S. Zhang, M. S. Smith, G. Arbanas, and R. L. Kozub, *Phys. Rev. C* **86**, 032802(R) (2012).
 [12] A. Aprahamian and Y. Sun, *Nat. Phys.* **1**, 81 (2005).
 [13] R. L. Lozeva *et al.*, *Phys. Rev. C* **77**, 064313 (2008).
 [14] A. Kankainen *et al.*, *Phys. Rev. C* **87**, 024307 (2013).
 [15] P. Walker and G. Dracoulis, *Nature (London)* **399**, 35 (1999).
 [16] A. Scherillo *et al.*, *Phys. Rev. C* **70**, 054318 (2004).
 [17] B. Fogelberg *et al.*, *Phys. Rev. C* **70**, 034312 (2004).

- [18] H. Grawe, K. Langanke, and G. Martínez-Pinedo, *Rep. Prog. Phys.* **70**, 1525 (2007).
- [19] H. Jin, M. Hasegawa, S. Tazaki, K. Kaneko, and Y. Sun, *Phys. Rev. C* **84**, 044324 (2011).
- [20] M. Hasegawa and K. Kaneko, *Phys. Rev. C* **59**, 1449 (1999).
- [21] M. Dufour and A. P. Zuker, *Phys. Rev. C* **54**, 1641 (1996).
- [22] J. Duflo and A. P. Zuker, *Phys. Rev. C* **59**, R2347 (1999).
- [23] L. S. Kisslinger and R. A. Sorensen, *Rev. Mod. Phys.* **35**, 853 (1963).
- [24] M. Baranger and K. Kumar, *Nucl. Phys. A* **110**, 490 (1968); **110**, 529 (1968); **122**, 241 (1968).
- [25] T. Kishimoto and T. Tamura, *Nucl. Phys. A* **192**, 246 (1972); **270**, 317 (1976).
- [26] M. Hasegawa, K. Kaneko, and S. Tazaki, *Nucl. Phys. A* **688**, 765 (2001).
- [27] K. Kaneko, M. Hasegawa, and T. Mizusaki, *Phys. Rev. C* **66**, 051306(R) (2002).
- [28] K. Kaneko, Y. Sun, M. Hasegawa, and T. Mizusaki, *Phys. Rev. C* **78**, 064312 (2008).
- [29] K. Kaneko, Y. Sun, T. Mizusaki, and M. Hasegawa, *Phys. Rev. C* **83**, 014320 (2011).
- [30] M. Hannawald *et al.*, *Phys. Rev. C* **62**, 054301 (2000).
- [31] W. Rae, NUSHELLX code, <http://knollhouse.org>.
- [32] M. Dworschak *et al.*, *Phys. Rev. Lett.* **100**, 072501 (2008).
- [33] B. Fogelberg and J. Blomqvist, *Nucl. Phys. A* **429**, 205 (1984).
- [34] B. A. Brown, N. J. Stone, J. R. Stone, I. S. Towner, and M. Hjorth-Jensen, *Phys. Rev. C* **71**, 044317 (2005).
- [35] J. M. Allmond *et al.*, *Phys. Rev. C* **87**, 054325 (2013).
- [36] <http://www.nndc.bnl.gov/ensdf/>.
- [37] Y. Khazov, I. Mitropolsky, and A. Rodionov, *Nucl. Data Sheets* **107**, 2715 (2006).
- [38] I. Dillmann *et al.*, *Phys. Rev. Lett.* **91**, 162503 (2003).
- [39] G. Martínez-Pinedo and K. Langanke, *Phys. Rev. Lett.* **83**, 4502 (1999).
- [40] T. Otsuka, T. Suzuki, M. Honma, Y. Utsuno, N. Tsunoda, K. Tsukiyama, and M. Hjorth-Jensen, *Phys. Rev. Lett.* **104**, 012501 (2010).